Environmental Science & Technology

Article

Cite This: Environ. Sci. Technol. 2019, 53, 8057−8067

pubs.acs.org/est

Springtime Nitrogen Oxide-Influenced Chlorine Chemistry in the Coastal Arctic

Stephen M. McNamara,[†] Angela R. W. Raso,[†,‡,$] Siyuan Wang,[†,▽] Sham Thanekar,[§] Eric J. Boone,[†,‡] Katheryn R. Kolesar,[†,◇] Peter K. Peterson,[†,○] William R. Simpson,[∥] Jose D. Fuentes,[§] Paul B. Shepson,[‡,⊥,◆] and Kerri A. Pratt*[,†,#]

[†]Department of Chemistry, University of Michigan, Ann Arbor, Michigan 48109, United States

[‡]Department of Chemistry, Purdue University, West Lafayette, Indiana 47907, United States

[§]Department of Meteorology and Atmospheric Science, Pennsylvania State University, University Park, Pennsylvania 16801, United States

[∥]Department of Chemistry and Biochemistry, University of Alaska Fairbanks, Fairbanks, Alaska 99775, United States

[⊥]Department of Earth, Atmospheric, and Planetary Sciences & Purdue Climate Change Research Center, Purdue University, West Lafayette, Indiana 47907, United States

[#]Department of Earth and Environmental Sciences, University of Michigan, Ann Arbor, Michigan 48109, United States

Supporting Information

ABSTRACT: Atomic chlorine (Cl) is a strong atmospheric oxidant that shortens the lifetimes of pollutants and methane in the springtime Arctic, where the molecular halogens Cl_2 and BrCl are known Cl precursors. Here, we quantify the contributions of reactive chlorine trace gases and present the first observations, to our knowledge, of $ClNO_2$ (another Cl precursor), N_2O_5, and HO_2NO_2 in the Arctic. During March − May 2016 near Utqiaġvik, Alaska, up to 21 ppt of $ClNO_2$, 154 ppt of Cl_2, 27 ppt of ClO, 71 ppt of N_2O_5, 21 ppt of BrCl, and 153 ppt of HO_2NO_2 were measured using chemical ionization mass spectrometry. The main Cl precursor was calculated to be Cl_2 (up to 73%) in March, while BrCl was a greater contributor (63%) in May, when total Cl production was lower. Elevated levels of $ClNO_2$, N_2O_5, Cl_2, and HO_2NO_2 coincided with pollution influence from the nearby town of Utqiaġvik and the North Slope of Alaska (Prudhoe Bay) Oilfields. We propose a coupled mechanism linking NO_x with Arctic chlorine chemistry. Enhanced Cl_2 was likely the result of the multiphase reaction of $Cl^-_{(aq)}$ with $ClONO_2$, formed from the reaction of ClO and NO_2. In addition to this NO_x-enhanced chlorine chemistry, Cl_2 and BrCl were observed under clean Arctic conditions from snowpack photochemical production. These connections between NO_x and chlorine chemistry, and the role of snowpack recycling, are important given increasing shipping and fossil fuel extraction predicted to accompany Arctic sea ice loss.

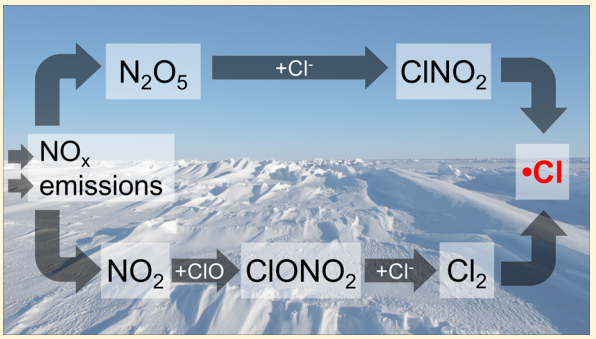

1. INTRODUCTION

The photolysis of atmospheric molecular chlorine (Cl_2), bromine chloride (BrCl), and nitryl chloride ($ClNO_2$) produces highly reactive chlorine (Cl) atoms that rapidly oxidize volatile organic compounds (VOCs), as well as the greenhouse gas methane.[1−3] Evidence of tropospheric chlorine chemistry has been observed in the Arctic region over the past decades. Early studies inferred atmospheric Cl levels, through measurements of VOC ratios and chlorinated VOCs (e.g., refs 4−8) ranging from 10^3−10^5 molecules cm^{-3} of Cl. Measurements of inorganic chlorine trace gases can also be used to provide estimates of ambient [Cl]. On the basis of observations of Cl_2, ClO, and BrCl, recent studies show numerically simulated Cl number densities reaching up to 10^6 molecules cm^{-3}, suggesting previous underestimates in [Cl].[9−11] Liao et al.[11] reported the first Arctic measurements of Cl_2 at up to 400 ppt (parts-per-trillion, pmol mol^{-1}) near Utqiaġvik (Barrow), AK in March−April 2009. Typically, Cl_2 is observed in the daytime and early evening and is correlated with ozone (O_3).[10,11] Custard et al.[12] observed photochemical production of Cl_2 and BrCl, similar to Br_2[13] and I_2,[14] from the coastal Arctic snowpack. Constrained by Cl_2 measurements from March 2012 near Utqiaġvik, ClO levels were simulated within measurement uncertainty, supporting Cl_2 as the primary

Received: March 25, 2019
Revised: June 1, 2019
Accepted: June 11, 2019
Published: June 11, 2019

DOI: 10.1021/acs.est.9b01797
Environ. Sci. Technol. 2019, 53, 8057−8067

Cl atom source during this period, yet other possible precursors were not measured for evaluation.[10]

Following Cl_2 photolysis (R1), Cl atoms react rapidly with VOCs or can react with O_3 to produce chlorine monoxide (ClO, R2).[1,4,15]

$$Cl_2 + h\nu\ (\lambda < 340\ nm) \rightarrow Cl + Cl \quad (R1)$$

$$Cl + O_3 \rightarrow ClO + O_2 \quad (R2)$$

The ClO can react with the hydroperoxy (HO_2) radical to produce hypochlorous acid (HOCl, R3).[1] Alternatively, ClO can react with nitrogen dioxide (NO_2) to produce chlorine nitrate ($ClONO_2$, R4).[1] Both HOCl and $ClONO_2$ can oxidize aqueous chloride (Cl^-) to regenerate Cl_2 (R5 and R6, respectively), or react with bromide to produce BrCl.[16,17]

$$ClO + HO_2 \rightarrow HOCl + O_2 \quad (R3)$$

$$ClO + NO_2 \rightarrow ClONO_2 \quad (R4)$$

$$HOCl + H^+_{(aq)} + Cl^-_{(aq)} \rightarrow Cl_2 + H_2O \quad (R5)$$

$$ClONO_2 + Cl^-_{(aq)} + H^+_{(aq)} \rightarrow Cl_2 + HNO_3 \quad (R6)$$

The formation of $ClONO_2$ is favored over HOCl in the springtime coastal Arctic troposphere, even for background levels of NO_2,[18] which are typically 10−100 ppt near Utqiaġvik,[19] up to 144 ppt at Ny Ålesund, Norway,[20] and up to 30 ppt at Alert, Canada.[21]

Chlorine atoms are also produced from the photolysis of nitryl chloride ($ClNO_2$), which is prevalent in the polluted midlatitude troposphere, measured at up to 1.0−8.3 ppb (parts-per-billion, nmol mol^{-1}) in coastal areas[22−26] and up to 0.1−1.5 ppb inland.[25,27−31] Dinitrogen pentoxide (N_2O_5), formed when NO_2 combines with the nitrate radical (NO_3) via reaction R7, undergoes heterogeneous reaction with aqueous chloride to form $ClNO_2$ (R8). In addition to being an important source of Cl atoms,[32] $ClNO_2$ also serves as a reservoir for nitrogen oxides (NO_x), producing NO_2 upon photolysis (R9).[1,15] The formation and loss processes of nitric oxide (NO), NO_2, and NO_3 are shown in R10−R12.[15]

$$NO_2 + NO_3 + M \rightleftharpoons N_2O_5 + M \quad (R7)$$

$$N_2O_5 + Cl^-_{(aq)} \rightarrow ClNO_2 + {NO_3}^-_{(aq)} \quad (R8)$$

$$ClNO_2 + h\nu\ (\lambda < 550\ nm) \rightarrow Cl + NO_2 \quad (R9)$$

$$NO + O_3 \rightarrow NO_2 + O_2 \quad (R10)$$

$$NO_2 + O_3 \rightarrow NO_3 + O_2 \quad (R11)$$

$$NO_3 + h\nu\ (\lambda < 690\ nm) \rightarrow NO + O_2 \quad (R12a)$$

$$\rightarrow NO_2 + O(^3P) \quad (R12b)$$

Notably, thermal and photolytic dissociation of N_2O_5 is slower under low temperature and reduced sunlight conditions, respectively,[33] characteristic of the springtime Arctic, in contrast to typical midlatitude conditions. In addition to $ClNO_2$ formation on aerosol surfaces,[34] N_2O_5 has been shown in the laboratory to react with chloride-doped ice surfaces to produce $ClNO_2$.[35] Since chloride is a dominant anion in the snowpack that is influenced by sea spray aerosol deposition,[36] the coastal Arctic snowpack may also serve as a source of $ClNO_2$.

In this work, we report the first Arctic measurements of $ClNO_2$, N_2O_5, and peroxynitric acid (HO_2NO_2), with concurrent Cl_2, ClO, and BrCl observations, using chemical ionization mass spectrometry (CIMS) from March 4 to May 20, 2016 near Utqiaġvik, Alaska, as part of the Photochemical Halogen and Ozone Experiment: Mass Exchange in the Lower Troposphere (PHOXMELT). Here, we investigate the conditions associated with observed enhanced chlorine chemistry. The influence of NO_x pollution and the proposed role of snowpack multiphase reactions are discussed. The observed chlorine atom precursors are used to calculate the Cl atom production rates during pollution periods, in comparison to background conditions, highlighting the role of NO_x in tropospheric chlorine chemistry with increasing Arctic development.

2. EXPERIMENTAL SECTION

2.1. Chemical Ionization Mass Spectrometry Measurements. Trace gas measurements were conducted at a tundra site southeast of Utqiaġvik, AK (71.275°N, 156.641°W) from March 4 to May 20, 2016 using CIMS (THS Instruments).[10,37] Briefly, the CIMS measures analytes by reaction with $I(H_2O)_n^-$ reagent ions, producing iodide adducts that are separated and detected by a quadrupole mass analyzer. The CIMS inlet, identical to previous campaigns,[10,12,37,38] consisted of a 30 cm long, 4.6 cm i.d. aluminum pipe with a stainless-steel ring torus attached to the outside end and extended 9 cm out of the building wall and ∼1 m above the snowpack. Approximately 300 L min^{-1} of air was pulled through the inlet and 6.6 L min^{-1} of this airflow was subsampled from the centerline into a 25 cm long, 0.65 cm i.d. PFA tube and through a 30 °C heated, custom three-way valve used for calibration and background measurements. The CIMS ion−molecule reaction region sampled 2.0 L min^{-1} of the inlet flow and was held at a constant pressure of 13 Torr. The $I(H_2O)_n^-$ reagent ions were produced by passing CH_3I (carried in N_2 at 1.7 L min^{-1}) through a ^{210}Po ionizer with water vapor (carried in N_2 at 0.12 L min^{-1}) added from a room temperature 1 L water bubbler. Humidifying the reaction chamber also prevented ambient water vapor from changing the CIMS sensitivity during ambient sampling.[37] All analyte signals were normalized to a measure of the reagent ion at m/z 147 ($IH_2{}^{18}O^-$) to account for minor fluctuations in H_2O addition (e.g., from fluctuations in water bubbler output) and detector sensitivity (Figure S1).

A list of the quantified species, their masses, and associated measurement uncertainties are listed in Table S1. The CIMS measurement cycle was 15 s, and it monitored 37 masses in total. Halogen species were positively identified using their measured isotopic ratios (additional details in Section S2 and Figure S2), and representative mass spectra are shown in Figure S3. Background measurements were conducted for 4 min every 15 min by passing the airflow through a glass wool scrubber, which removed molecular halogen species,[37,39] as well as $ClNO_2$, N_2O_5, and HO_2NO_2, with >95% efficiency (Figure S4). Between March 4 and May 8, N_2O_5 was quantified at m/z 235 using hourly mass scans (100 ms dwell time) before it was added to the CIMS mass list. Details of the N_2O_5 mass scans are discussed in Figure S5. After April 8, instrument background signals for nitric acid (HNO_3) were sufficiently low for quantitation. Calibrations of Cl_2 and Br_2 in the field were conducted every 2 h by adding 0.12 L min^{-1} of Cl_2 or Br_2 in N_2 (2.6 ± 0.4 ppb and 1.3 ± 0.3 ppb,

DOI: 10.1021/acs.est.9b01797
Environ. Sci. Technol. 2019, 53, 8057−8067

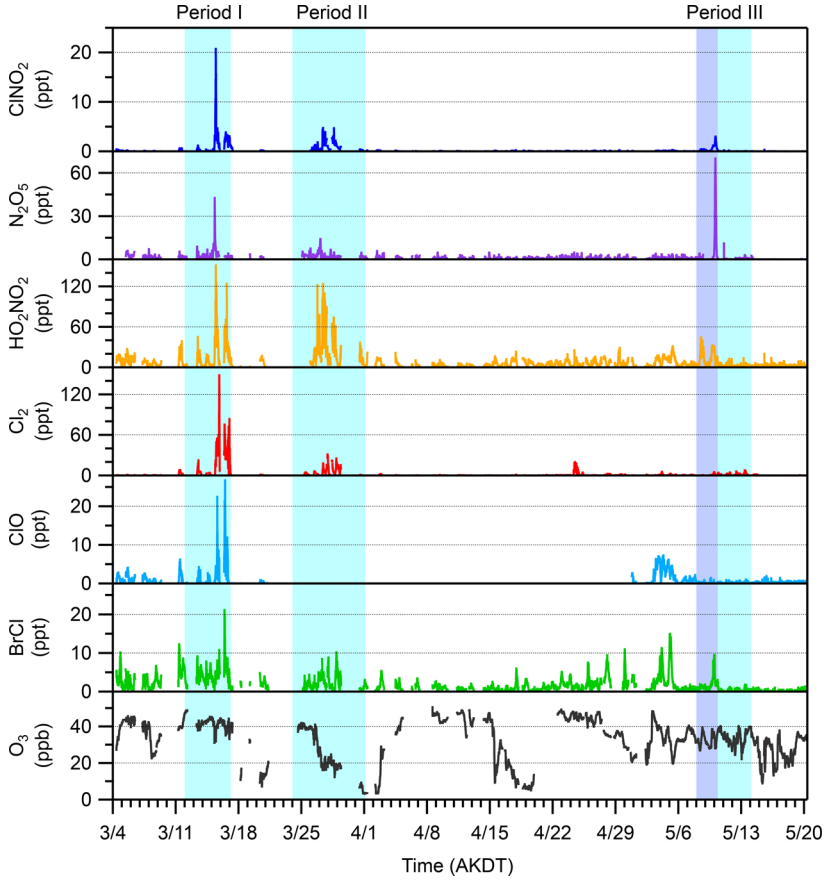

Figure 1. Time series of $ClNO_2$, N_2O_5, HO_2NO_2, Cl_2, ClO, BrCl, and O_3 mole ratios for March 4−May 20, 2016 measured at the CIMS field site near Utqiaġvik. The three periods of pollution influence from the town of Utqiaġvik, as defined in Identification of Pollution Influenced Periods, are shaded blue. Period III includes a period of air mass influence from the North Slope of Alaska oilfields (purple shading). ClO could not be quantified due to a mass interference between March 25−April 30 and is not shown for that period.

respectively), from individual permeation sources (VICI Metronics, Inc.) to the CIMS inlet flow. The permeation rates were verified daily by bubbling the Cl_2 or Br_2 flows into 2% potassium iodide solutions and measuring the oxidation product, triiodide (I_3^-), with UV−visible spectrophotometry at 352 nm.[37] All other species ($ClNO_2$, N_2O_5, ClO, BrCl, HO_2NO_2, HNO_3) were calibrated offline with sensitivities relative to Cl_2 or Br_2 (Table S1). Details of the offline calibration procedures are described in Section S3. Table S1 lists the 3σ limits of detection (LODs), corresponding to 4 min background periods, and the 10 min averaged 3σ LODs to account for variations in the 4 min background expected due to counting statistics.[37] The measurement uncertainties listed in Table S1 include the propagated uncertainties in the Cl_2 and Br_2 calibrations, fluctuation in the CIMS background signals, and uncertainty in the relative sensitivity factor (when applicable). All average mole ratios are reported with 95% confidence intervals.

2.2. Nitrogen Oxides (NO and NO_2) and Additional Auxiliary Measurements. To identify the influence of pollution at the field site, nitrogen oxides (NO and NO_2) and wind (speed and direction) were measured during PHOXMELT. Nitric oxide (NO) was measured at the CIMS field site intermittently from March 10 to May 19, 2016, with the gaps in data coverage due to instrument−data logger communication issues. At 10 m above the snowpack, air was pulled through a 25 m long, 0.8 cm i.d. PFA tube at a flow rate of 10−15 L min^{-1} into a manifold from which the Thermo Scientific NO_x analyzer (model 42i) subsampled. To assess general NO_x levels when in situ NO measurements were unavailable, nitrogen dioxide (NO_2) differential slant column densities (dSCDs) were measured continuously throughout the campaign using multiaxis differential optical absorption spectroscopy (MAX-DOAS).[40] The MAX-DOAS instrument was located ∼14 m above the ground on the roof of the Barrow Arctic Research Center (BARC, 71.325°N, 156.668°W), ∼6 km north of the CIMS field site across flat tundra (Figure S6), and its viewing azimuth was 23° east of north. The MAX-DOAS measures NO_2 along its entire detection path (up to ∼15 km, depending on visibility),[41] which includes air over the Beaufort Sea and NO_2 emitted in the Utqiaġvik vicinity. NO_2 dSCDs were obtained using previously published methods.[41,42] Ozone (O_3) was measured using an O_3 monitor (2B Technologies, model 205) that subsampled at 1.3 L min^{-1} from the CIMS inlet (6.6 L min^{-1} total inlet flow as described in Chemical Ionization Mass Spectrometry Measurements). Additional NO, NO_2, and O_3 measurement details are shown in Table S1.

For March 4−17, solar radiation (at ∼6.5 m above ground level) and wind speed and direction (at 10 m) data were obtained from the NOAA Barrow Observatory (71.3230°N, 156.6114°W, https://www.esrl.noaa.gov/gmd/obop/brw/) located ∼6 km north of the field site across flat tundra. Wind speed and direction were also measured at the CIMS field site at ∼11.5 m above ground level, and solar radiation was measured at ∼3 m above ground level, from March 17 to May

DOI: 10.1021/acs.est.9b01797
Environ. Sci. Technol. 2019, 53, 8057−8067

20. Gaps in the meteorological data (such as March 21−24 due to a power outage at the field site) are supplemented by the NOAA measurements. Photolysis rate constants for Cl_2, $ClNO_2$, and BrCl on March 15, March 27, and May 9−10 were calculated using the Tropospheric, Ultraviolet, and Visible (TUV) Radiation Model 5.3.1. (https://www2.acom.ucar.edu/modeling/tropospheric-ultraviolet-and-visible-tuv-radiation-model). Daily atmospheric sounding data from the Wiley Post-Will Rogers Memorial Airport (PABR) were used to estimate boundary layer height (http://weather.uwyo.edu/upperair/sounding.html).

2.3. Identification of Pollution Influenced Periods. Using observations of NO, NO_2, and wind direction, days with pollution influence were classified according to the following criteria: (1) For at least half of the day, winds came from the 120°−360° direction, corresponding to the town of Utqiaġvik and its outskirts (including a gravel mine located ∼1 km south of the field site). (2) NO or NO_2 were observed above their respective instrument LODs (0.4 ppb and 2.5×10^{15} molecules cm^{-2}, respectively), consistent with previous classifications of background NO_x (0.01−0.1 ppb)[19] and polluted (>0.7 ppb)[43] conditions at Utqiaġvik. Days when Hybrid Single Particle Lagrangian Integrated Trajectory (HYSPLIT) 72 h backward air mass trajectories showed transport from the North Slope of Alaska (Prudhoe Bay) oilfields (Figure S7) were also considered to be pollution influenced (discussed further in North Slope of Alaska (Prudhoe Bay) Oilfields Influence). In total, 19 of the 77 days during PHOXMELT were classified as "Polluted": March 12−16 (period I), March 24−31 (period II), and May 8−13 (period III) (Figures 1, 2A). Two days did not meet all criteria but were classified as polluted: enhanced NO and NO_2 were observed on March 12 (period I) despite not having winds from pollution-influenced areas for at least half of the day, and March 14 (within period I) had north−northwest winds from Utqiaġvik, but NO and NO_2 were below LODs. From April 2 to May 11 (including a portion of period III, Figure 2A), NO observations were unavailable. However, MAX-DOAS NO_2 dSCDs were enhanced (8 times above LOD) on May 9 and 10, further supporting pollution influence during period III (Figures 2A, S8).

3. RESULTS AND DISCUSSION

3.1. Three Periods of Enhanced Chlorine Chemistry Coincide with NO_x Pollution Influence. During spring over the snow-covered tundra near Utqiaġvik, enhanced mole ratios of trace chlorine-containing gases, particularly Cl_2 and $ClNO_2$, were observed during three polluted periods (defined in Identification of Pollution Influenced Periods) occurring in mid-March, late-March, and mid-May 2016 (Figures 1, S8). During these periods, winds came from pollution-influenced areas (120°−360°), including the town of Utqiaġvik, and NO and NO_2 levels were highest, with NO typically reaching 1 to 3 ppb during the day (Figures 2A, S6, S8). This is far above Arctic background NO mole ratios of 0.01−0.1 ppb previously observed during spring in Utqiaġvik.[19] Levels of Cl_2 and $ClNO_2$ peaked on March 15, reaching 154 and 21 ppt, respectively (Figures 1, S8). During the three periods, O_3 was typically >20 ppb (near background levels of 30−40 ppb)[44,45] when Cl_2 was elevated (Figures 1, S9), consistent with previous studies showing higher Cl_2 levels in the presence of O_3.[10,11,18,46] Additionally, NO_x reservoir species N_2O_5 (precursor to $ClNO_2$) and peroxynitric acid (HO_2NO_2) were only observed during these three polluted periods (Figures 1, S8), with N_2O_5 ranging from 15 to 71 ppt and HO_2NO_2 ranging from 30 to 153 ppt.

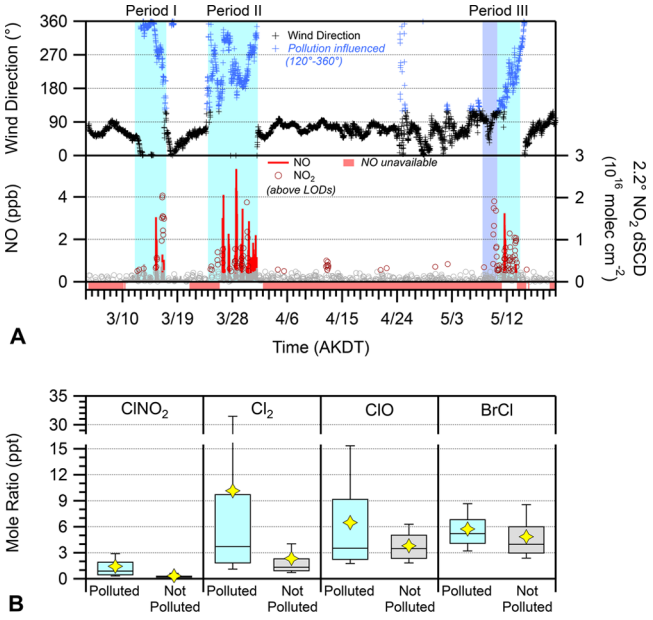

Figure 2. (A) March 4−May 20, 2016 time series of wind direction (top panel) and in situ NO mole ratios and MAX-DOAS NO_2 differential slant column densities (dSCDs) (bottom panel). NO and NO_2 data shown in gray are below instrument limits of detection (NO: 0.4 ppb; NO_2: 2.5×10^{15} molecules cm^{-2}). Red shading (bottom) denotes periods when NO measurements were unavailable. Measurement data in panel A were used to classify the Polluted periods (light blue shading). May 8−10, during period III, was influenced by the North Slope of Alaska oilfields (light purple shading, Figure S7). (B) Box and whisker plots showing the distributions (90th/10th and 75th/25th percentiles, and medians) of $ClNO_2$, Cl_2, ClO, and BrCl measurements binned by days classified as Polluted vs Not Polluted. The yellow star represents the mean of each population. Only $ClNO_2$, Cl_2, ClO, and BrCl mole ratios above their respective LODs are included in the distributions.

Outside of the polluted periods, $ClNO_2$ and Cl_2 were predominantly below the CIMS LODs (0.3 and 0.8 ppt, respectively). Winds came from the northeast and east across the Beaufort Sea, representing Arctic background conditions;[47] as such, NO and NO_2 were below their respective LODs due to limited pollution influence (Figures 2A, S6, S8). An exception was April 24−25 when Cl_2 reached 21 ppt; this period is consistent with previous observations of photochemical snowpack Cl_2 production under Arctic background NO_x conditions.[10−12] During the daytime of March 16 in period I, ClO reached 27 ppt when Cl_2 was 62 ppt (Figures 1, S8); however, due to a mass interference, ClO could not be quantified from March 25 to April 30 and was below the CIMS LOD for period III. Additionally, BrCl was observed during polluted periods (up to 21 ppt in period I) and up to 15 ppt outside of the polluted periods (Figure 1), consistent with previously observed snowpack production[12] and coupling with bromine chemistry.[11,48]

Mole ratios of $ClNO_2$, Cl_2, ClO, and BrCl were examined as a function of polluted and not polluted days (Figure 2B). For polluted days, $ClNO_2$, Cl_2, ClO, and BrCl mole ratios were all statistically higher ($p < 0.05$) than during the nonpolluted days (outside of the three polluted periods). In particular, little $ClNO_2$ was observed during the nonpolluted days (average of 0.33 ± 0.01 ppt, Figure 2B), as expected, due to a lack of

DOI: 10.1021/acs.est.9b01797
Environ. Sci. Technol. 2019, 53, 8057−8067

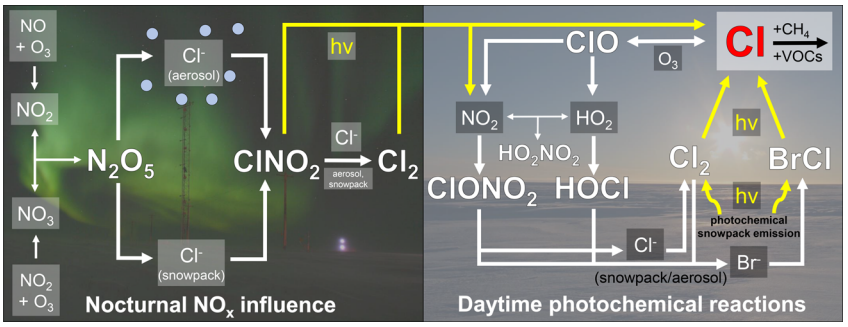

Figure 3. Overview of proposed coupled Arctic chlorine and NO_x chemistry, from both daytime photochemically driven reactions and nighttime dark reactions. NO_x is emitted from combustion sources (Figure S6) and daytime snowpack photochemistry.[62−65] Direct photochemical production of Cl_2 and BrCl from the coastal Arctic snowpack during the daytime has been previously observed.[12] The formation of $ClNO_2$ on the snowpack as well as the subsequent oxidation of $Cl^-_{(aq)}$ (under acidic conditions) and $Br^-_{(aq)}$ (not shown here) are hypothesized based on previous laboratory studies.[57−59] Previous numerical modeling of background springtime Arctic conditions suggests $ClONO_2 + Cl^-_{(aq)}$ can account for over 50% of total Cl_2 production, with the remainder due to direct snowpack emission.[18]

sufficient NO_x for formation of N_2O_5 (R7, 10−12), which was below the CIMS LOD during the nonpolluted days. Likewise, the highest observations of Cl_2 occurred during the three polluted periods (average, 10.2 ± 0.4 ppt), while lower Cl_2 mole ratios (average, 2.3 ± 0.1 ppt) were observed during the nonpolluted periods (Figure 2B). For previous Cl_2 observations by Liao et al.,[11] the nearby field site was also periodically influenced by air from nearby Utqiaġvik, and the observed Cl_2 was not correlated with pollutants such as NO, carbon monoxide, or benzene. Similarly, the Cl_2 observed in this campaign was also not directly correlated with NO (R^2 = 0.004, Figure S10); however, this relationship does not consider additional Cl_2 production and recycling pathways involving chlorinated NO_x derivatives such as $ClONO_2$, as discussed in Arctic Chlorine Production Mechanisms and Connection to the Snowpack. The enhancement of ClO and BrCl during the polluted days is not as strong (Figure 2B) due to additional controlling factors. The enhanced chlorine species observed during the three periods were not a result of boundary layer height variations (no correlation observed, Figure S11) and were not correlated with winds from the local waste incinerator (327° with respect to the field site), ruling out a direct halogen emission source.[30]

3.2. North Slope of Alaska (Prudhoe Bay) Oilfields Influence. From May 8 00:00 to May 10 05:00 AKDT (UTC-8 h, during period III), 72 h backward air mass trajectories show transport to Utqiaġvik from the North Slope of Alaska (Prudhoe Bay) oilfields, a prominent NO_x emission source about 330 km to the southeast[49,50] (Figure S7, Identification of Pollution Influenced Periods). During this time, local winds were predominantly from the east and southeast, consistent with the modeled air mass trajectories (Figure S7). Winds began to shift more westerly through May 10 and May 11, reverting to local NO_x influence (from Utqiaġvik) for the remainder of period III (Figure S7). This oilfield influenced period was characterized by elevated $ClNO_2$ and Cl_2, as well as the highest N_2O_5 mole ratio (71 ppt) observed, during the night of May 9−10. Additional NO_y species, HO_2NO_2 and nitric acid (HNO_3), were observed during the evenings of May 8 and May 9 at up to 30−40 and 500 ppt, respectively (Figures 1, S8, S12). May 8−10 was the only period for which substantial HNO_3 (>100 ppt) was observed (Figure S12). Therefore, it is likely that the elevated NO_y species, $ClNO_2$, N_2O_5, HNO_3, and HO_2NO_2, measured near Utqiaġvik were the result of NO_x emissions from the oilfields to the southeast. HO_2NO_2 decomposes at higher temperatures, leading to longer lifetimes under colder conditions. The lifetime of HO_2NO_2 for the observed temperatures (−10 °C to −1 °C) during May 8−10 is ∼6 min, based on approximations in Murphy et al.,[51] suggesting that formation and recycling of HO_2NO_2 during transport via $HO_2 + NO_2 \rightleftharpoons HO_2NO_2$ would explain the observations. This is consistent with previous observations by Jaffe et al.[49] of elevated levels of NO_y near Utqiaġvik when under Prudhoe Bay Oilfield air mass influence. Measurements of HO_2NO_2 are sparse, with previous observations in the free troposphere,[52] midlatitude oilfields in the wintertime,[53] and the Antarctic.[54,55] To our knowledge, the HO_2NO_2 observations here represent the first in the Arctic atmospheric boundary layer. The presence of $ClNO_2$, N_2O_5, HO_2NO_2, and HNO_3 due to transport of Prudhoe Bay air masses to Utqiaġvik highlights the regional scale influence of NO_x and its impact on chlorine chemistry and tropospheric oxidants in the Arctic.

3.3. Arctic Chlorine Production Mechanisms and Connection to the Snowpack. Figure 3 summarizes the proposed connections between NO_x pollution and Arctic chlorine chemistry. NO_2 is required for the formation of N_2O_5 (R7), which reacts in the dark on chlorine-containing aerosols to produce $ClNO_2$ (R8) and is a well-known chlorine activation pathway in midlatitude regions.[22,27,32,56] Also proposed is the production of $ClNO_2$ from the reaction of N_2O_5 on chloride-containing ice (snow) surfaces, as shown in the laboratory.[35] The $ClNO_2$ was only observed during the three polluted periods (Figures 1, 2, S8), when N_2O_5 was above the CIMS LOD (Table S1). Laboratory studies have also demonstrated the oxidation of aqueous bromide by $ClNO_2$, forming BrCl under neutral pH conditions.[57,58] Under highly acidic (pH < 2) conditions, $ClNO_2$ has been shown to react with aerosol Cl^- to form Cl_2.[59] However, most $ClNO_2$ is expected to undergo photolysis to produce chlorine atoms that react with hydrocarbons.[1] A fraction of the Cl atoms reacts with O_3 to produce the observed ClO (R2), which reacts with HO_2 to produce HOCl (R3) or NO_2 to generate $ClONO_2$ (R4). Wang and Pratt[18] showed that even at background NO_2 conditions of 0.01−0.1 ppb near Utqiaġvik, $ClONO_2$ formation (R4) is up to five times more favored than HOCl production (R3). Therefore, during the polluted days, $ClONO_2$ production would be even further favored. Laboratory studies have shown that $ClONO_2$ reacts with chloride-containing surfaces to produce Cl_2 (R6),[17,34]

DOI: 10.1021/acs.est.9b01797
Environ. Sci. Technol. 2019, 53, 8057−8067

suggesting the potential for aerosol and snowpack Cl_2 formation via $ClONO_2$ reaction. Since O_3 is required for $ClONO_2$ production, depleted O_3 conditions (<10 ppb) should inhibit this pathway, as demonstrated by near zero Cl_2 levels on March 31 during period II when O_3 was 3−10 ppb (Figure S8). Under background springtime Arctic conditions near Utqiaġvik, previous numerical model simulations suggest that the $ClONO_2 + Cl^-_{(aq)}$ reaction (R6) may serve as a major snowpack Cl_2 source, accounting for over half of the total Cl_2 production.[18] The remainder of Cl_2 is simulated to be directly emitted from the snowpack,[18] as previously observed,[12] via the oxidation of $Cl^-_{(aq)}$ by condensed phase hydroxyl radicals (OH),[60] similar to snowpack Br_2 production.[12−14,60] Additionally, the reaction of $ClONO_2$ with $Br^-_{(aq)}$ has been shown to produce BrCl in the laboratory,[17,61] and this may explain the observed elevated BrCl during the three polluted periods (Figures 1, 2, S8). The snowpack is also a daytime source of NO_x and condensed phase OH, through the photolysis of nitrate and nitrite,[62−65] and likely facilitates $ClONO_2$ production. $ClONO_2$ reaction with chloride could explain the Cl_2 enhancement observed during the polluted periods.

3.4. Distinct $ClNO_2$ and Cl_2 Diel Profiles. Here, we discuss the distinct diel behavior of $ClNO_2$ and Cl_2 observed during the three polluted periods (Figure 4). Rapid photolysis

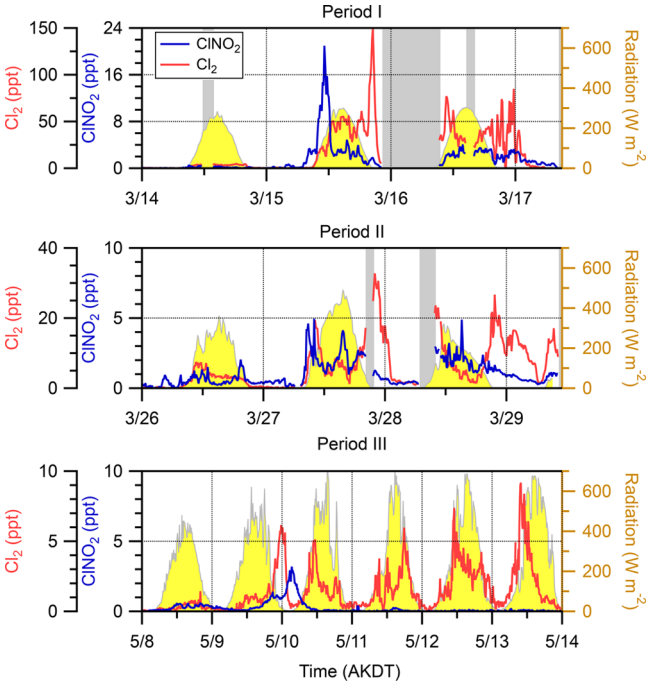

Figure 4. Time series of $ClNO_2$ and Cl_2 mole ratios with measured solar radiation, illustrating distinct diel patterns during the three pollution-influenced periods. Gray shading represents periods for which CIMS data are unavailable.

upon sunrise generally restricts $ClNO_2$ to the night and early morning in the midlatitudes,[24] but during periods I and II, $ClNO_2$ persisted up to 4 ppt throughout the afternoons of March 15, 16, 27, and 28. Early spring in the Arctic experiences reduced solar radiation, with observed maxima of 200−400 W m^{-2} (Figure 4) and lower solar elevation angles (maxima of 17°−22° in March), resulting in weaker photolysis. Longer photolytic lifetimes in the early Arctic spring (3.7 h on March 15 12:00 AKDT; 2.6 h on March 27 12:00 AKDT) compared to the midlatitudes (less than 1 h)[31] can explain the daytime $ClNO_2$. Daytime persistence of $ClNO_2$ has been observed previously in heavily polluted regions in the midlatitudes after breakdown of the nocturnal boundary layer and in-flow of polluted air masses from aloft.[66,67] However, the Arctic boundary layer over the cold, snow-covered ground is generally stable and long-lived.[68] Further, extreme low temperatures below the eutectic point of $NaCl{\cdot}2H_2O$ (−22 °C)[69] were observed during periods I and II (−30 °C to −25 °C) and may have decreased the availability of Cl^- for reaction with N_2O_5,[12,70] delaying $ClNO_2$ production until sunrise when temperatures increased (−20 °C to −15 °C, Figure S13). The observed Cl_2 diel profile, peaking in the morning and early evening, was generally consistent with previous springtime Arctic observations (Figure 4).[10,11,18] Previously, <0.8 ppt Cl_2 was typically observed after midnight near Utqiaġvik by Liao et al.[11] and Custard et al.,[10] and our observations were generally consistent with these previous studies. A notable exception was March 29, when Cl_2 levels remained at 10−16 ppt for several hours past midnight. Reaction of $ClNO_2$ with an acidic chloride-containing surface[59] (Arctic Chlorine Production Mechanisms and Connection to the Snowpack, Figure 3) could provide a nocturnal Cl_2 production pathway and possibly explain the Cl_2 observed during the night.

3.5. Contributions of $ClNO_2$, Cl_2, and BrCl Photolysis to Cl Atom Production Rates. The comprehensive suite of chlorine trace gas measurements during spring 2016 allows further examination of additional Cl atom precursors, expanding upon the work of Custard et al.,[10] which focused solely on Cl_2 during background NO_x conditions. Figure 5 shows the calculated Cl atom production rates (P_{Cl}) for $ClNO_2$, Cl_2, and BrCl photolysis during a subset of the three polluted periods (March 15, March 27, and May 9−10). Total P_{Cl} was highest on March 15, reaching 0.13 ppt s^{-1} at 15:00 when solar radiation was near its peak, in comparison to 0.032 ppt s^{-1} maximum on March 27 and 0.018 ppt s^{-1} maximum on May 9−10. The maximum P_{Cl} on March 15 is due to the higher observed daytime levels of Cl_2, with a maximum of 55 ppt Cl_2 at 14:30, compared to 18 ppt on March 27 and 6 ppt on May 9−10. For comparison, the maximum P_{Cl} observed in this study (0.13 ppt s^{-1} or 3.7 × 10^6 molecules cm^{-3} s^{-1}) is approximately six times faster than the maximum P_{Cl} estimated in the Los Angeles area (0.64 × 10^6 molecules cm^{-3} s^{-1}),[23] likely due to the larger contribution from daytime Cl_2 photolysis during PHOXMELT. In contrast, Liu et al.[46] reported a maximum modeled P_{Cl} of 1 ppb h^{-1}, or 0.28 ppt s^{-1}, for high levels of daytime Cl_2 on the North China Plain (typically >100 ppt), resulting in a faster P_{Cl} from Cl_2 photolysis.

In all three cases, Cl_2 photolysis contributed significantly to the total P_{Cl}, amounting to 72.7% on March 15, 49.1% on March 27, and 36.5% on May 9−10 (Figure 5). Maximum Cl_2 photolysis frequencies (J_{Cl2}) were calculated to be between 0.9 to 2.1 × 10^{-3} s^{-1}, corresponding to photolytic lifetimes of 8 to 19 min. The photolysis of BrCl was also a major driver of P_{Cl}, particularly on May 9−10 during period III (63% contribution), when Cl_2 mole ratios were <6 ppt. BrCl photolyzes faster than Cl_2, with maxima in J_{BrCl} between 5 to 11 × 10^{-3} s^{-1}, which correspond to photolysis lifetimes of only 1 to 3 min. $ClNO_2$ contributed minimally to the total P_{Cl}, with the maximum P_{Cl} due to $ClNO_2$ photolysis reaching 0.0007 ppt s^{-1} at 11:30 on March 15 when observed $ClNO_2$ mole ratios were

DOI: 10.1021/acs.est.9b01797
Environ. Sci. Technol. 2019, 53, 8057−8067

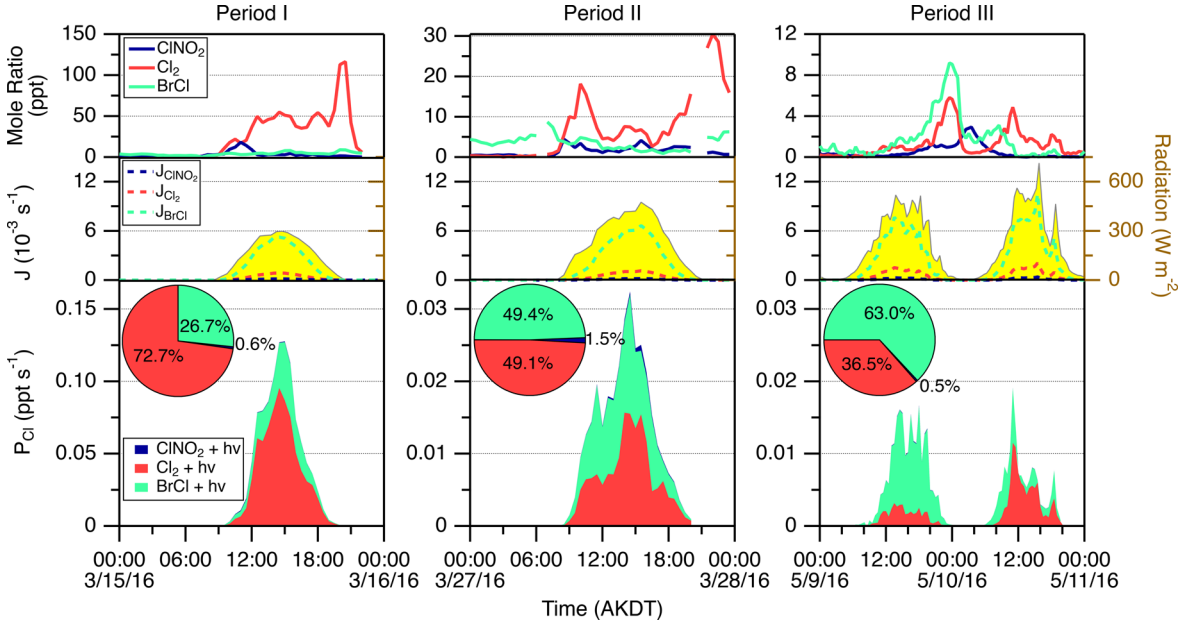

Figure 5. (Top) 30 min averaged $ClNO_2$, Cl_2, and BrCl mole ratios measured by CIMS on March 15, March 27, and May 9−10, 2016 (periods I, II, and III). (Middle) Photolysis frequencies for $ClNO_2$, Cl_2, and BrCl were calculated using the outputs of a radiative transfer model and scaled to measured solar radiation. (Bottom) Calculated chlorine atom production rates (P_{Cl}) from photolysis of measured $ClNO_2$ (minor contribution), Cl_2, and BrCl. Pie charts show the integrated contributions to P_{Cl}.

the highest (21 ppt). Overall, $ClNO_2$ photolysis contributed only 0.5 to 1.5% to P_{Cl} during the three periods. Maxima in calculated J_{ClNO2} ranged from 0.1 to 0.4 × 10^{-3} s^{-1}, corresponding to much longer lifetimes of 42 to 167 min for $ClNO_2$. Despite the low P_{Cl} from $ClNO_2$, the Cl atoms generated from $ClNO_2$ photolysis may participate in additional chlorine recycling reactions, subsequently enhancing the production of Cl_2 (Figure 3).

Outside of the three NO_x polluted periods, Cl_2 and $ClNO_2$ averaged just 2.3 ± 0.1 and 0.33 ± 0.01 ppt, respectively (Figure 2B). For context, the Cl_2 mole ratios observed during background conditions in this study (up to 21 ppt) were lower than previous observations (up to 400 ppt) near Utqiaġvik.[10−12] For the maximum J_{Cl} of 2.1 × 10^{-3} s^{-1} from Figure 5, this corresponds to a P_{Cl} of up to 0.01 ppt s^{-1} for Arctic background Cl_2, an order of magnitude lower than the P_{Cl} of 0.10 ppt s^{-1} from Cl_2 on March 15. Considering the maximum J_{ClNO2} of 0.4 × 10^{-3} s^{-1}, a maximum Arctic background P_{Cl} of 0.0001 ppt s^{-1} is expected from $ClNO_2$. This is approximately seven times lower than the maximum P_{Cl} from $ClNO_2$ on March 15 (0.0007 ppt s^{-1}). P_{Cl} due to BrCl photolysis, given the maximum J_{BrCl} of 11 × 10^{-3} s^{-1}, was similar between polluted (0.06 ppt s^{-1} for average BrCl of 5.8 ± 0.1 ppt) and background conditions (0.05 ppt s^{-1} for average BrCl of 4.9 ± 0.1 ppt), highlighting additional controls on BrCl production due to its coupling with reactive bromine chemistry.[11,48] Overall, chlorine atom production from Cl_2 and $ClNO_2$ during the polluted periods (average maximum P_{Cl} of 0.04 ppt s^{-1}) was approximately four times faster than that for Arctic background periods (maximum P_{Cl} of 0.01 ppt s^{-1}, Figure 5). In addition to this enhancement of the chlorine atom production rate, these results also suggest that Cl_2 is the most important contributor to the production of Cl atoms during the spring.

3.6. Atmospheric Implications. The results from the spring 2016 Arctic field campaign highlight the influence of NO_x on the production of Cl atom precursors, particularly Cl_2 and $ClNO_2$. Given the episodic nature of the observed chlorine species, with maxima occurring during NO_x-polluted conditions, we propose that NO_x promotes the production of $ClNO_2$ and Cl_2, which subsequently influences the Cl atom budget. This proposed NO_x-influenced chlorine activation mechanism is in addition to previously observed photochemical Cl_2 snowpack production under clean conditions.[12] Currently, $ClNO_2$ plays a minor role in the production of Cl atoms (0.5−1.5% of P_{Cl}) under enhanced NO_x conditions, but as shipping and fossil fuel extraction continue to increase in the Arctic,[71] $ClNO_2$ abundance will likely increase, potentially increasing Cl atom production through photolysis and possible Cl_2 production from reaction on acidic chloride-containing surfaces. High levels of $ClNO_2$ may exist in other Arctic locations with elevated NO_x emissions and influence from sea spray aerosol, such as the Russian and Norwegian Arctic, where oil and gas production, as well as shipping, are predicted to increase.[71,72] During the polar night, $ClNO_2$ could build up due to its long nocturnal lifetime, allowing for its transport throughout the Arctic region, as shown by our observations of enhanced HO_2NO_2, $ClNO_2$, and N_2O_5 during May 8−10 when winds came from Prudhoe Bay. Additional studies near and downwind of major Arctic NO_x emission sources, many of which are often overlooked,[73] are needed during the polar night and at polar sunrise to examine this potential regional impact.

We propose a coupled mechanism connecting NO_x pollution and snowpack chlorine chemistry. Enhanced Cl_2 during high NO_x periods, leading to faster Cl atom production, may result from $ClONO_2$ production via reaction of ClO and NO_2, produced from combustion emissions and photochemical snowpack production via nitrate and nitrite photolysis.[62−65] $ClNO_2$ is hypothesized to form from the reaction of N_2O_5 with snowpack Cl^-, in addition to aerosol Cl^-. $ClNO_2$ and N_2O_5 flux measurements above the snowpack

DOI: 10.1021/acs.est.9b01797
Environ. Sci. Technol. 2019, 53, 8057−8067

are needed to confirm this pathway. $ClNO_2$ may participate in additional halogen cycling reactions such as the oxidation of Cl^- to Cl_2 (on acidic surfaces)[59] and Br^- to BrCl.[57,58] More laboratory studies are needed (e.g., on frozen surfaces) to examine the potential for Cl^- and Br^- oxidation by $ClNO_2$ within the snowpack under relevant Arctic conditions. In situ measurements of $ClONO_2$ are required to assess its potential contribution to Cl_2 recycling during high NO_x conditions. In addition, the impacts of a wide range of NO_x levels should be evaluated through field measurements at Arctic locations more directly affected by NO_x pollution, including oilfields and high-latitude cities, given increasing development.[73]

■ ASSOCIATED CONTENT

Supporting Information

The Supporting Information is available free of charge on the ACS Publications website at DOI: 10.1021/acs.est.9b01797.

Overview of CIMS, O_3, and NO_x measurements and figures of merit; CIMS reagent ion signal during ambient sampling; isotopic ratio plots for Cl_2, $ClNO_2$, ClO, and BrCl (10 min averaged) for all days and polluted-only days; representative mass spectra for Cl_2, HO_2NO_2, $ClNO_2$, N_2O_5, and BrCl; performance of the CIMS glass wool background scrubber; comparison of the N_2O_5 mass scan and selected ion monitoring data; identification of halogen species using isotopic ratios; offline calibration procedures for $ClNO_2$, N_2O_5, ClO, BrCl, HO_2NO_2, and HNO_3; NO and NO_2 wind rose plots, and description of sampling sites; representative HYSPLIT backward air mass trajectories and measurements of wind speed/direction to show influence from the North Slope of Alaska oilfields; trace gas observations during the three polluted periods; observations of relationship between Cl_2 and O_3; Cl_2 mole ratios vs NO mole ratios; vertical potential temperature measurements from daily soundings at Utqiaġvik; HNO_3 measurements from April 8−May 20, 2016; $ClNO_2$ and N_2O_5 mole ratios, air temperature, and solar radiation measurements during the three polluted periods (PDF)

■ AUTHOR INFORMATION

Corresponding Author

*E-mail: prattka@umich.edu. Phone: (734) 763-2871.

ORCID

Peter K. Peterson: 0000-0002-9337-6677

Kerri A. Pratt: 0000-0003-4707-2290

Present Addresses

[$]W.R.: New Mexico Environment Department, Santa Fe, NM, U.S.A.

[▽]S.W.: National Center for Atmospheric Research, Boulder, CO, U.S.A.

[◊]K.R.K.: Air Sciences Inc., Portland, OR, U.S.A.

[○]P.K.P.: Department of Chemistry, Whittier College, Whittier, CA, U.S.A.

[◆]P.B.S.: School of Marine & Atmospheric Sciences, Stony Brook University, Stony Brook, NY, U.S.A.

Notes

The authors declare no competing financial interest.

PHOXMELT CIMS data are archived and available for download from the National Science Foundation Arctic Data Center (https://arcticdata.io/catalog/view/doi:10.18739/A2ZC7RT62).

■ ACKNOWLEDGMENTS

Financial support was provided by the National Science Foundation Arctic Natural Sciences program (PLR-1417668, PLR-1417906, PLR-1417914) and the National Aeronautics and Space Administration Earth Science Program (NNX14AP44G). We thank Ukpeaġvik Iñupiat Corporation-Science and PolarField Services, as well as Dandan Wei and Jesus Ruiz-Plancarte (Pennsylvania State University), for fieldwork support in Utqiaġvik. The NOAA ESRL GMD (http://esrl.noaa.gov/gmd/) is acknowledged for wind and solar radiation data from the Barrow Observatory. Surface albedo data were obtained from the NSA ARM Climate Research Facility, a U.S. DOE Office of Science user facility sponsored by the Office of Biological and Environmental Research. We thank Hans Osthoff (University of Calgary) for discussions of the $ClNO_2$ calibration, L. Gregory Huey and David Tanner (Georgia Institute of Technology) for loan of the NO analyzer, and Tom Ryerson and Chelsea Thompson (NOAA) for loan of the NO_2 converter used for CIMS calibrations.

■ REFERENCES

(1) Simpson, W. R.; Brown, S. S.; Saiz-Lopez, A.; Thornton, J. A.; von Glasow, R. Tropospheric Halogen Chemistry: Sources, Cycling, and Impacts. *Chem. Rev.* **2015**, *115*, 4035−4062.

(2) Young, C. J.; Washenfelder, R. A.; Edwards, P. M.; Parrish, D. D.; Gilman, J. B.; Kuster, W. C.; Mielke, L. H.; Osthoff, H. D.; Tsai, C.; Pikelnaya, O.; Stutz, J.; Veres, P. R.; Roberts, J. M.; Griffith, S.; Dusanter, S.; Stevens, P. S.; Flynn, J. H.; Grossberg, N.; Lefer, B. L.; Holloway, J. S.; Peischl, J.; Ryerson, T. B.; Atlas, E.; Blake, D. R.; Brown, S. S. Chlorine as a Primary Radical: Evaluation of Methods to Understand Its Role in Initiation of Oxidative Cycles. *Atmos. Chem. Phys.* **2014**, *14* (7), 3427−3440.

(3) Lawler, M. J.; Sander, R.; Carpenter, L. J.; Lee, J. D.; von Glasow, R.; Sommariva, R.; Saltzman, E. S. HOCl and Cl2 Observations in Marine Air. *Atmos. Chem. Phys.* **2011**, *11* (15), 7617−7628.

(4) Jobson, B. T.; Niki, H.; Yokouchi, Y.; Bottenheim, J. W.; Hopper, F.; R, L. Measurements of C2-C6 Hydrocarbons during the Polar Sunrise 1992 Experiment: Evidence for Cl Atom and Br Atom Chemistry. *J. Geophys. Res.* **1994**, *99* (D12), 5355−25368.

(5) Impey, G. A.; Shepson, P. B.; Hastie, D. R.; Barrie, L. A.; Anlauf, K. G. Measurements of Photolyzable Chlorine and Bromine during the Polar Sunrise Experiment 1995. *J. Geophys. Res.* **1997**, *102* (D13), 5−10.

(6) Ariya, P. A.; Jobson, B. T.; Sander, R.; Niki, H.; Harris, G. W.; Hopper, J. F.; Anlauf, K. G. Measurements of C2 -C7 Hydrocarbons during the Polar Sunrise Experiment 1994: Further Evidence for Halogen Chemistry in the Troposphere. *J. Geophys. Res. Atmos.* **1998**, *103* (D11), 13169−13180.

(7) Keil, A. D.; Shepson, P. B. Chlorine and Bromine Atom Ratios in the Springtime Arctic Troposphere as Determined from Measurements of Halogenated Volatile Organic Compounds. *J. Geophys. Res.* **2006**, *111* (17), 1−11.

(8) Tackett, P. J.; Cavender, A. E.; Keil, A. D.; Shepson, P. B.; Bottenheim, J. W.; Morin, S.; Deary, J.; Steffen, A.; Doerge, C. A Study of the Vertical Scale of Halogen Chemistry in the Arctic Troposphere during Polar Sunrise at Barrow, Alaska. *J. Geophys. Res.* **2007**, *112* (7), 1−13.

(9) Stephens, C. R.; Shepson, P. B.; Steffen, A.; Bottenheim, J. W.; Liao, J.; Huey, L. G.; Apel, E. C.; Weinheimer, A. J.; Hall, S. R.; Cantrell, C. A.; Sive, B. C.; Knapp, D. J.; Montzka, D. D.; Hornbrook, R. S. The Relative Importance of Chlorine and Bromine Radicals in

DOI: 10.1021/acs.est.9b01797
Environ. Sci. Technol. 2019, 53, 8057−8067

the Oxidation of Atmospheric Mercury at Barrow, Alaska. *J. Geophys. Res. Atmos.* **2012**, *117* (5), 1−16.
(10) Custard, K. D.; Pratt, K. A.; Wang, S.; Shepson, P. B. Constraints on Arctic Atmospheric Chlorine Production through Measurements and Simulations of Cl2 and ClO. *Environ. Sci. Technol.* **2016**, *50*, 12394−12400.
(11) Liao, J.; Huey, L. G.; Liu, Z.; Tanner, D. J.; Cantrell, C. A.; Orlando, J. J.; Flocke, F. M.; Shepson, P. B.; Weinheimer, A. J.; Hall, S. R.; Ullmann, K.; Beine, H. J.; Wang, Y.; Ingall, E. D.; Stephens, C. R.; Hornbrook, R. S.; Apel, E. C.; Riemer, D. D.; Fried, A.; Mauldin, R. L.; Smith, J. N.; Staebler, R. M.; Neuman, J. A.; Nowak, J. B. High Levels of Molecular Chlorine in the Arctic Atmosphere. *Nat. Geosci.* **2014**, *7* (2), 91−94.
(12) Custard, K. D.; Raso, A. R. W.; Shepson, P. B.; Staebler, R. M.; Pratt, K. A. Production and Release of Molecular Bromine and Chlorine from the Arctic Coastal Snowpack. *Earth Sp. Chem.* **2017**, *1* (3), 142−151.
(13) Pratt, K. A.; Custard, K. D.; Shepson, P. B.; Douglas, T. A.; Pöhler, D.; General, S.; Zielcke, J.; Simpson, W. R.; Platt, U.; Tanner, D. J.; Gregory Huey, L.; Carlsen, M.; Stirm, B. H. Photochemical Production of Molecular Bromine in Arctic Surface Snowpacks. *Nat. Geosci.* **2013**, *6* (5), 351−356.
(14) Raso, A. R. W.; Custard, K. D.; May, N. W.; Tanner, D. J.; Newburn, M. K.; Walker, L.; Moore, R. J.; Huey, L. G.; Alexander, L.; Shepson, P. B.; Pratt, K. A. Active Molecular Iodine Photochemistry in the Arctic. *Proc. Natl. Acad. Sci. U. S. A.* **2017**, *114* (38), 10053−10058.
(15) Burkholder, J. B.; Sander, S. P.; Abbatt, J. P. D.; Barker, J. R.; Huie, R. E.; Kolb, C. E.; Kurylo, M. J.; Orkin, V. L.; Wilmouth, D. M.; Wine, P. H. Chemical Kinetics and Photochemical Data for Use in Atmospheric Studies, Evaluation No. 18. *JPL Publ.* **2015**, *15* (10), 1−153.
(16) Abbatt, J. P. D.; Molina, M. J. The Heterogoenous Reaction of HOCl + HCl -> Cl2 + H2O on Ice and Nitric Acid Trihydrate: Reaction Probabilities and Stratospheric Implications. *Geophys. Res. Lett.* **1992**, *19* (5), 461−464.
(17) Deiber, G.; George, C.; Le Calvé, S.; Schweitzer, F.; Mirabel, P. Uptake Study of ClONO2 and BrONO2 by Halide Containing Droplets. *Atmos. Chem. Phys.* **2004**, *4* (5), 1291−1299.
(18) Wang, S.; Pratt, K. A. Molecular Halogens Above the Arctic Snowpack: Emissions, Diurnal Variations, and Recycling Mechanisms. *J. Geophys. Res. Atmos.* **2017**, *122* (21), 11991−12007.
(19) Villena, G.; Wiesen, P.; Cantrell, C. A.; Flocke, F. M.; Fried, A.; Hall, S. R.; Hornbrook, R. S.; Knapp, D. J.; Kosciuch, E.; Mauldin, R. L.; McGrath, J. A.; Montzka, D.; Richter, D.; Ullmann, K.; Walega, J.; Weibring, P.; Weinheimer, A. J.; Staebler, R. M.; Liao, J.; Huey, L. G.; Kleffmann, J. Nitrous Acid (HONO) during Polar Spring in Barrow, Alaska: A Net Source of OH Radicals? *J. Geophys. Res.* **2011**, *116* (24), 1−12.
(20) Beine, H. J.; Jaffe, D. A.; Stordal, F.; Engardt, M.; Solberg, S.; Schmidbauer, N.; Holmen, K. NOx during Ozone Depletion Events in the Arctic Troposphere at Ny-Alesund, Svalbard. *Tellus, Ser. B* **1997**, *49*, 556−565.
(21) Muthuramu, K.; Shepson, P. B.; Bottenheim, J. W.; Jobson, B. T.; Niki, H.; Anlauf, K. G. Relationships between Organic Nitrates and Surface Ozone Destruction during Polar Sunrise Experiment 1992. *J. Geophys. Res.* **1994**, *99* (D12), 25369.
(22) Osthoff, H. D.; Roberts, J. M.; Ravishankara, A. R.; Williams, E. J.; Lerner, B. M.; Sommariva, R.; Bates, T. S.; Coffman, D. J.; Quinn, P. K.; Dibb, J. E.; Stark, H.; Burkholder, J. B.; Talukdar, R. K.; Meagher, J. F.; Fehsenfeld, F. C.; Brown, S. S. High Levels of Nitryl Chloride in the Polluted Subtropical Marine Boundary Layer. *Nat. Geosci.* **2008**, *1* (5), 324−328.
(23) Riedel, T. P.; Bertram, T. H.; Crisp, T. A.; Williams, E. J.; Lerner, B. M.; Vlasenko, A.; Li, S. M.; Gilman, J. B.; de Gouw, J. A.; Bon, D. M.; Wagner, N. L.; Brown, S. S.; Thornton, J. A. Nitryl Chloride and Molecular Chlorine in the Coastal Marine Boundary Layer. *Environ. Sci. Technol.* **2012**, *46* (19), 10463−10470.
(24) Mielke, L. H.; Stutz, J.; Tsai, C.; Hurlock, S. C.; Roberts, J. M.; Veres, P. R.; Froyd, K. D.; Hayes, P. L.; Cubison, M. J.; Jimenez, J. L.; Washenfelder, R. A.; Young, C. J.; Gilman, J. B.; de Gouw, J. A.; Flynn, J. H.; Grossberg, N.; Lefer, B. L.; Liu, J.; Weber, R. J.; Osthoff, H. D. Heterogeneous Formation of Nitryl Chloride and Its Role as a Nocturnal NOx Reservoir Species during CalNex-LA 2010. *J. Geophys. Res. Atmos.* **2013**, *118* (18), 10638−10652.
(25) Wang, T.; Tham, Y. J.; Xue, L.; Li, Q.; Zha, Q.; Wang, Z.; Poon, S. C. N.; Dubé, W. P.; Blake, D. R.; Louie, P. K. K.; Luk, C. W. Y.; Tsui, W.; Brown, S. S. Observations of Nitryl Chloride and Modeling Its Source and Effect on Ozone in the Planetary Boundary Layer of Southern China. *J. Geophys. Res. Atmos.* **2016**, *121*, 2476−2489.
(26) Yun, H.; Wang, W.; Wang, T.; Xia, M.; Yu, C.; Wang, Z.; Poon, S.; Yue, D.; Zhou, Y. Nitrate Formation from Heterogeneous Uptake of Dinitrogen Pentoxide during a Severe Winter Haze in Southern China. *Atmos. Chem. Phys.* **2018**, *18* (23), 17515−17527.
(27) Thornton, J. A.; Kercher, J. P.; Riedel, T. P.; Wagner, N. L.; Cozic, J.; Holloway, J. S.; Dubé, W. P.; Wolfe, G. M.; Quinn, P. K.; Middlebrook, A. M.; Alexander, B.; Brown, S. S. A Large Atomic Chlorine Source Inferred from Mid-Continental Reactive Nitrogen Chemistry. *Nature* **2010**, *464* (7286), 271−274.
(28) Mielke, L. H.; Furgeson, A.; Osthoff, H. D. Observation of $ClNO_2$ in a Mid-Continental Urban Environment. *Environ. Sci. Technol.* **2011**, *45* (20), 8889−8896.
(29) Mielke, L. H.; Furgeson, A.; Odame-Ankrah, C. A.; Osthoff, H. D. Ubiquity of ClNO2 in the Urban Boundary Layer of Calgary, Alberta, Canada. *Can. J. Chem.* **2016**, *94*, 414−423.
(30) Riedel, T. P.; Wagner, N. L.; Dubé, W. P.; Middlebrook, A. M.; Young, C. J.; Öztürk, F.; Bahreini, R.; Vandenboer, T. C.; Wolfe, D. E.; Williams, E. J.; Roberts, J. M.; Brown, S. S.; Thornton, J. A. Chlorine Activation within Urban or Power Plant Plumes: Vertically Resolved $ClNO_2$ and Cl_2 Measurements from a Tall Tower in a Polluted Continental Setting. *J. Geophys. Res. Atmos.* **2013**, *118* (15), 8702−8715.
(31) Phillips, G. J.; Tang, M. J.; Thieser, J.; Brickwedde, B.; Schuster, G. L.; Bohn, B.; Lelieveld, J.; Crowley, J. N. Significant Concentrations of Nitryl Chloride Observed in Rural Continental Europe Associated with the Influence of Sea Salt Chloride and Anthropogenic Emissions. *Geophys. Res. Lett.* **2012**, *39* (10), 1−5.
(32) Sarwar, G.; Simon, H.; Xing, J.; Mathur, R. Importance of Tropospheric ClNO2 Chemistry across the Northern Hemisphere. *Geophys. Res. Lett.* **2014**, *41* (11), 4050−4058.
(33) Chang, W. L.; Bhave, P. V.; Brown, S. S.; Riemer, N.; Stutz, J.; Dabdub, D. Heterogeneous Atmospheric Chemistry, Ambient Measurements, and Model Calculations of N2O5: A Review. *Aerosol Sci. Technol.* **2011**, *45* (6), 665−695.
(34) Finlayson-Pitts, B. J.; Ezell, M. J.; Pitts, J. N. Formation of Chemically Active Chlorine Compounds by Reactions of Atmospheric NaCl Particles with Gaseous N2O5 and ClONO2. *Nature* **1989**, *337* (6204), 241−244.
(35) Lopez-Hilfiker, F.; Constantin, K.; Kercher, J. P.; Thornton, J. A. Temperature Dependent Halogen Activation by N2O5 Reactions on Halide-Doped Ice Surfaces. *Atmos. Chem. Phys.* **2012**, *12* (11), 5237−5247.
(36) Krnavek, L.; Simpson, W. R.; Carlson, D.; Dominé, F.; Douglas, T. A.; Sturm, M. The Chemical Composition of Surface Snow in the Arctic: Examining Marine, Terrestrial, and Atmospheric Influences. *Atmos. Environ.* **2012**, *50* (4), 349−359.
(37) Liao, J.; Sihler, H.; Huey, L. G.; Neuman, J. A.; Tanner, D. J.; Friess, U.; Platt, U.; Flocke, F. M.; Orlando, J. J.; Shepson, P. B.; Beine, H. J.; Weinheimer, A. J.; Sjostedt, S. J.; Nowak, J. B.; Knapp, D. J.; Staebler, R. M.; Zheng, W.; Sander, R.; Hall, S. R.; Ullmann, K. A Comparison of Arctic BrO Measurements by Chemical Ionization Mass Spectrometry and Long Path-Differential Optical Absorption Spectroscopy. *J. Geophys. Res.* **2011**, *116*, D00R02.
(38) Liao, J.; Huey, L. G.; Tanner, D. J.; Flocke, F. M.; Orlando, J. J.; Neuman, J. A.; Nowak, J. B.; Weinheimer, A. J.; Hall, S. R.; Smith, J. N.; Fried, A.; Staebler, R. M.; Wang, Y.; Koo, J. H.; Cantrell, C. A.;

DOI: 10.1021/acs.est.9b01797
Environ. Sci. Technol. 2019, 53, 8057−8067

Weibring, P.; Walega, J.; Knapp, D. J.; Shepson, P. B.; Stephens, C. R. Observations of Inorganic Bromine (HOBr, BrO, and Br2) Speciation at Barrow, Alaska, in Spring 2009. *J. Geophys. Res. Atmos.* **2012**, *117* (6), 1−11.
(39) Neuman, J. A.; Nowak, J. B.; Huey, L. G.; Burkholder, J. B.; Dibb, J. E.; Holloway, J. S.; Liao, J.; Peischl, J.; Roberts, J. M.; Ryerson, T. B.; Scheuer, E.; Stark, H.; Stickel, R. E.; Tanner, D. J.; Weinheimer, A. J. Bromine Measurements in Ozone Depleted Air over the Arctic Ocean. *Atmos. Chem. Phys.* **2010**, *10* (14), 6503−6514.
(40) Hönninger, G.; von Friedeburg, C.; Platt, U. Multi Axis Differential Optical Absorption Spectroscopy (MAX-DOAS). *Atmos. Chem. Phys.* **2004**, *4* (1), 231−254.
(41) Peterson, P. K.; Simpson, W. R.; Pratt, K. A.; Shepson, P. B.; Frieß, U.; Zielcke, J.; Platt, U.; Walsh, S. J.; Nghiem, S. V. Dependence of the Vertical Distribution of Bromine Monoxide in the Lower Troposphere on Meteorological Factors Such as Wind Speed and Stability. *Atmos. Chem. Phys.* **2015**, *15* (4), 2119−2137.
(42) Simpson, W. R.; Peterson, P. K.; Frieß, U.; Sihler, H.; Lampel, J.; Platt, U.; Moore, C.; Pratt, K. A.; Shepson, P. B.; Halfacre, J.; Nghiem, S. V. Horizontal and Vertical Structure of Reactive Bromine Events Probed by Bromine Monoxide MAX-DOAS. *Atmos. Chem. Phys.* **2017**, *17* (15), 9291−9309.
(43) Custard, K. D.; Thompson, C. R.; Pratt, K. A.; Shepson, P. B.; Liao, J.; Huey, L. G.; Orlando, J. J.; Weinheimer, A. J.; Apel, E. C.; Hall, S. R.; Flocke, F. M.; Mauldin, R. L.; Hornbrook, R. S.; Pöhler, D.; General, S.; Zielcke, J.; Simpson, W. R.; Platt, U.; Fried, A.; Weibring, P.; Sive, B. C.; Ullmann, K.; Cantrell, C. A.; Knapp, D. J.; Montzka, D. D. The NOx Dependence of Bromine Chemistry in the Arctic Atmospheric Boundary Layer. *Atmos. Chem. Phys.* **2015**, *15* (18), 10799−10809.
(44) Helmig, D.; Oltmans, S. J.; Carlson, D.; Lamarque, J. F.; Jones, A.; Labuschagne, C.; Anlauf, K.; Hayden, K. A Review of Surface Ozone in the Polar Regions. *Atmos. Environ.* **2007**, *41* (24), 5138−5161.
(45) Oltmans, S. J.; Johnson, B. J.; Harris, J. M. Springtime Boundary Layer Ozone Depletion at Barrow, Alaska: Meteorological Influence, Year-to-Year Variation, and Long-Term Change. *J. Geophys. Res. Atmos.* **2012**, *117* (8), 1−18.
(46) Liu, X.; Qu, H.; Huey, L. G.; Wang, Y.; Sjostedt, S.; Zeng, L.; Lu, K.; Wu, Y.; Hu, M.; Shao, M.; Zhu, T.; Zhang, Y. High Levels of Daytime Molecular Chlorine and Nitryl Chloride at a Rural Site on the North China Plain. *Environ. Sci. Technol.* **2017**, *51* (17), No. 9588.
(47) Quinn, P. K.; Miller, T. L.; Bates, T. S.; Ogren, J. A.; Andrews, E.; Shaw, G. E. A 3-Year Record of Simultaneously Measured Aerosol Chemical and Optical Properties at Barrow, Alaska. *J. Geophys. Res. Atmos.* **2002**, *107* (D11), AAC 8−1.
(48) Foster, K. L.; Plastridge, R. A.; Bottenheim, J. W.; Shepson, P. B.; Finlayson-Pitts, B. J.; Spicer, C. W. The Role of Br2 and BrCl in Surface Ozone Destruction at Polar Sunrise. *Science* **2001**, *291* (1990), 471−474.
(49) Jaffe, D. A.; Honrath, R. E.; Furness, D.; Conway, T. J.; Dlugokencky, E. J.; Steele, L. P. A Determination of the CH4, NOx and CO2 Emissions from the Prudhoe Bay, Alaska Oil Development. *J. Atmos. Chem.* **1995**, *20* (3), 213−227.
(50) Jaffe, D. A.; Honrath, R. E.; Herring, J. A.; Li, S. M.; Kahl, J. D. Measurements of Nitrogen-Oxides at Barrow, Alaska during Spring - Evidence for Regional and Northern Hemispheric Sources of Pollution. *J. Geophys. Res.* **1991**, *96* (D4), 7395−7405.
(51) Murphy, J. G.; Thornton, J. A.; Wooldridge, P. J.; Day, D. A.; Rosen, R. S.; Cantrell, C. A.; Shetter, R. E.; Lefer, B.; Cohen, R. C. Measurements of the Sum of HO2NO2 and CH3O2NO2 in the Remote Troposphere. *Atmos. Chem. Phys.* **2004**, *4* (2), 377−384.
(52) Kim, S.; Huey, L. G.; Stickel, R. E.; Tanner, D. J.; Crawford, J. H.; Olson, J. R.; Chen, G.; Brune, W. H.; Ren, X.; Lesher, R.; Wooldridge, P. J.; Bertram, T. H.; Perring, A.; Cohen, R. C.; Lefer, B. L.; Shetter, R. E.; Avery, M.; Diskin, G.; Sokolik, I. Measurement of HO2NO2 in the Free Troposphere during the Intercontinental Chemical Transport Experiment - North America 2004. *J. Geophys. Res.* **2007**, *112* (12), 1−10.
(53) Veres, P. R.; Roberts, J. M.; Wild, R. J.; Edwards, P. M.; Brown, S. S.; Bates, T. S.; Quinn, P. K.; Johnson, J. E.; Zamora, R. J.; de Gouw, J. A. Peroxynitric Acid (HO2NO2) Measurements during the UBWOS 2013 and 2014 Studies Using Iodide Ion Chemical Ionization Mass Spectrometry. *Atmos. Chem. Phys.* **2015**, *15* (14), 8101−8114.
(54) Slusher, D. L.; Haman, B. J.; Tanner, D. J.; Huey, L. G. A Chemical Ionization Technique for Measurement of Pernitric Acid in the Upper Troposphere and the Polar Boundary Layer. *Geophys. Res. Lett.* **2001**, *28* (20), 3875−3878.
(55) Slusher, D. L.; Huey, L. G.; Tanner, D. J.; Chen, G.; Davis, D. D.; Buhr, M.; Nowak, J. B.; Eisele, F. L.; Kosciuch, E.; Mauldin, R. L.; Lefer, B. L.; Shetter, R. E.; Dibb, J. E. Measurements of Pernitric Acid at the South Pole during ISCAT 2000. *Geophys. Res. Lett.* **2002**, *29* (21), 7-1.
(56) Li, Q.; Zhang, L.; Wang, T.; Tham, Y. J.; Ahmadov, R.; Xue, L.; Zhang, Q.; Zheng, J. Impacts of Heterogeneous Uptake of Dinitrogen Pentoxide and Chlorine Activation on Ozone and Reactive Nitrogen Partitioning: Improvement and Application of WRF-Chem Model in Southern China. *Atmos. Chem. Phys.* **2016**, *16*, 14875−14890.
(57) Fickert, S.; Helleis, F.; Adams, J. W.; Moortgat, G. K.; Crowley, J. N. Reactive Uptake of ClNO2 on Aqueous Bromide Solutions. *J. Phys. Chem. A* **1998**, *102* (52), 10689−10696.
(58) Frenzel, A.; Scheer, V.; Sikorski, R.; George, C.; Behnke, W.; Zetzsch, C. Heterogeneous Interconversion Reactions of BrNO2, ClNO2, Br 2, and Cl2. *J. Phys. Chem. A* **1998**, *102* (8), 1329−1337.
(59) Roberts, J. M.; Osthoff, H. D.; Brown, S. S.; Ravishankara, A. R. N2O5 Oxidizes Chloride to Cl2 in Acidic Atmospheric Aerosol. *Science* **2008**, *321*, 1059.
(60) Halfacre, J. W.; Shepson, P. B.; Pratt, K. A. PH-Dependent Production of Molecular Chlorine, Bromine, and Iodine from Frozen Saline Surfaces. *Atmos. Chem. Phys.* **2019**, *19* (7), 4917−4931.
(61) Aguzzi, A.; Rossi, M. J. The Kinetics of the Heterogeneous Reaction of BrONO2 with Solid Alkali Halides at Ambient Temperature. A Comparison with the Interaction of ClONO2 on NaCl and KBr. *Phys. Chem. Chem. Phys.* **1999**, *1* (18), 4337−4346.
(62) France, J. L.; Reay, H. J.; King, M. D.; Voisin, D.; Jacobi, H. W.; Dominé, F.; Beine, H. J.; Anastasio, C.; MacArthur, A.; Lee-Taylor, J. Hydroxyl Radical and NOx Production Rates, Black Carbon Concentrations and Light-Absorbing Impurities in Snow from Field Measurements of Light Penetration and Nadir Reflectivity of Onshore and Offshore Coastal Alaskan Snow. *J. Geophys. Res. Atmos.* **2012**, *117* (D14), 1−21.
(63) Honrath, R. E.; Lu, Y.; Peterson, M. C.; Dibb, J. E.; Arsenault, M. A.; Cullen, N. J.; Steffen, K. Vertical Fluxes of NOx, HONO, and HNO3 above the Snowpack at Summit, Greenland. *Atmos. Environ.* **2002**, *36* (15−16), 2629−2640.
(64) Honrath, R. E.; Jaffe, D. A. The Seasonal Cycle of Nitrogen Oxides in the Arctic Troposphere at Barrow, Alaska. *J. Geophys. Res.* **1992**, *97* (D18), 20615.
(65) Honrath, R. E.; Peterson, M. C.; Guo, S.; Shepson, P. B.; Campbell, B. Evidence of NOx Production Within or Upon Ice Particles in the Greenland Snowpack. *Geophys. Res. Lett.* **1999**, *26* (6), 695−698.
(66) Le Breton, M.; Hallquist, Å. M.; Pathak, R. K.; Simpson, D.; Wang, Y.; Johansson, J.; Zheng, J.; Yang, Y.; Shang, D.; Wang, H.; Liu, Q.; Chan, C.; Wang, T.; Bannan, T. J.; Priestley, M.; Percival, C. J.; Shallcross, D. E.; Lu, K.; Guo, S.; Hu, M.; Hallquist, M. Chlorine Oxidation of VOCs at a Semi-Rural Site in Beijing: Significant Chlorine Liberation from ClNO2 and Subsequent Gas and Particle Phase Cl-VOC Production. *Atmos. Chem. Phys.* **2018**, *18*, 13013−13030.
(67) Tham, Y. J.; Wang, Z.; Li, Q.; Yun, H.; Wang, W.; Wang, X.; Xue, L.; Lu, K.; Ma, N.; Bohn, B.; Li, X.; Kecorius, S.; Größ, J.; Shao, M.; Wiedensohler, A.; Zhang, Y.; Wang, T. Significant Concentrations of Nitryl Chloride Sustained in the Morning: Investigations of the Causes and Impacts on Ozone Production in a Polluted Region of Northern China. *Atmos. Chem. Phys.* **2016**, *16*, 14959−14977.

DOI: 10.1021/acs.est.9b01797
Environ. Sci. Technol. 2019, 53, 8057−8067

(68) Anderson, P. S.; Neff, W. D. Boundary Layer Physics over Snow and Ice. *Atmos. Chem. Phys.* **2008**, *8* (13), 3563−3582.
(69) Koop, T.; Kapilashrami, A.; Molina, L. T.; Molina, M. J. Phase Transitions of Sea-Salt/Water Mixtures at Low Temperatures: Implications for Ozone Chemistry in the Polar Marine Boundary Layer. *J. Geophys. Res.* **2000**, *105* (D21), 26393−26402.
(70) Sjostedt, S. J.; Abbatt, J. P. D. Release of Gas-Phase Halogens from Sodium Halide Substrates: Heterogeneous Oxidation of Frozen Solutions and Desiccated Salts by Hydroxyl Radicals. *Environ. Res. Lett.* **2008**, *3* (4), 045007.
(71) Peters, G. P.; Nilssen, T. B.; Lindholt, L.; Eide, M. S.; Glomsrød, S.; Eide, L. I.; Fuglestvedt, J. S. Future Emissions from Shipping and Petroleum Activities in the Arctic. *Atmos. Chem. Phys.* **2011**, *11* (11), 5305−5320.
(72) Roiger, A.; Thomas, J. L.; Schlager, H.; Law, K. S.; Kim, J.; Schäfler, A.; Weinzierl, B.; Dahlkötter, F.; Risch, I. K.; Marelle, L.; Minikin, A.; Raut, J. C.; Reiter, A.; Rose, M.; Scheibe, M.; Stock, P.; Baumann, R.; Bouarar, I.; Lerbaux, C. C.; George, M.; Onishi, T.; Flemming, A. J. Quantifying Emerging Local Anthropogenic Emissions in the Arctic Region: The Access Aircraft Campaign Experiment. *Bull. Am. Meteorol. Soc.* **2015**, *96* (3), 441−460.
(73) Schmale, J.; Arnold, S. R.; Law, K. S.; Thorp, T.; Anenberg, S.; Simpson, W. R.; Mao, J.; Pratt, K. A. Local Arctic Air Pollution: A Neglected but Serious Problem. *Earth's Future* **2018**, *6* (10), 1385.

DOI: 10.1021/acs.est.9b01797
Environ. Sci. Technol. 2019, 53, 8057−8067